Vaccine 37 (2019) 6405–6414

Contents lists available at ScienceDirect

Vaccine

journal homepage: www.elsevier.com/locate/vaccine

Virus-like particle-display of the enterotoxigenic *Escherichia coli* heat-stable toxoid STh-A14T elicits neutralizing antibodies in mice

Morten L. Govasli [a,1], Yuleima Diaz [a], Pål Puntervoll [a,b,*]

[a] NORCE Norwegian Research Centre, Postboks 22 Nygårdstangen, 5838 Bergen, Norway
[b] Centre for International Health, Department of Global Public Health and Primary Care, University of Bergen, Postboks 7804, 5020 Bergen, Norway

ARTICLE INFO

Article history:
Received 14 May 2019
Received in revised form 30 August 2019
Accepted 2 September 2019
Available online 9 September 2019

Keywords:
ETEC
Enterotoxin
Heat-stable toxin
ST
Subunit vaccine
Virus-like particles

ABSTRACT

Enterotoxigenic *Escherichia coli* (ETEC) causes diarrhoea by secreting enterotoxins into the small intestine. Human ETEC strains may secrete any combination of three enterotoxins: the heat-labile toxin (LT) and the heat-stable toxins (ST), of which there are two variants, called human ST (STh) and porcine ST (STp). Strains expressing STh, either alone or in combination with LT and/or STp, are among the four most important diarrhoea-causing pathogens affecting children in low- and middle-income countries. ST is therefore an attractive target for ETEC vaccine development. To produce a safe ST-based vaccine, several challenges must be solved. ST must be rendered immunogenic and non-toxic, and antibodies elicited by an ST vaccine should neutralize ST but not cross-react with the endogenous ligands uroguanylin and guanylin. Virus-like particles (VLPs) tend to be highly immunogenic and are increasingly being used as carriers for presenting heterologous antigens in new vaccines. In this study, we have coupled native STh and the STh-A14T toxoid to the coat protein of Acinetobacter phage AP205 by using the SpyCatcher system and immunized mice with these VLPs without the use of adjuvants. We found that both STs were efficiently coupled to the VLP, that both the STh and STh-A14T VLPs were immunogenic in mice, and that the resulting serum antibodies could completely neutralize the toxic activities of native STh. The serum antibodies showed a high degree of immunological cross-reaction to STp, while there was little or no unwanted cross-reaction to uroguanylin and guanylin. Moreover, compared to native STh, the STh-A14T mutation did not seem to negatively impact the immunogenicity of the construct or the neutralizing ability of the resulting sera. Taken together, these findings demonstrate that VLPs are suitable carriers for making STs immunogenic, and that the STh-A14T-coupled AP205 VLP represents a promising ETEC vaccine candidate.

1. Introduction

Diarrheal diseases caused by infections with enterotoxigenic *Escherichia coli* (ETEC) is a major contributor to health problems among young children living in low- and middle-income countries (LMICs) [1–5] and for travellers visiting these countries [6]. Diarrhoea may lead to malnutrition in young children, especially when they experience repeated or prolonged diarrhoeal episodes. ETEC contributes to this child undernutrition, which in turn makes children more vulnerable to other serious infections [7]. ETEC's negative impact on global health and its consequent negative economic impact suggest that a vaccine against ETEC should be prioritized [8,9]. To date no ETEC-specific vaccines are available [10].

ETEC is predominantly transmitted through faecal contamination of food and water [11]. Following oral ingestion, ETEC colonizes the small intestine, and diarrhoea is induced by the secretion of one, two, or all of three different enterotoxins: the heat-labile enterotoxin (LT), the human heat-stable enterotoxin (STh), and the porcine heat-stable enterotoxin (STp) [11]. STh and STp are 18 and 19 amino acid peptides, respectively, and they are 78% identical [12]. ETEC strains secreting STh are among the four most important pathogens associated with moderate-to-severe diarrhoea in LMIC children [13], making STh one of the most attractive targets for ETEC vaccine development.

STh and STp, which are commonly referred to as ST, bind to and activate the transmembrane guanylyl cyclase C (GC-C) receptor,

Abbreviations: ETEC, Enterotoxigenic *Escherichia coli*; ST, heat-stable toxin; VLP, virus-like particle.

* Corresponding author at: NORCE Norwegian Research Centre, Postboks 22 Nygårdstangen, 5838 Bergen, Norway.
E-mail address: pal.puntervoll@norceresearch.no (P. Puntervoll).
[1] Present address: Division of Infection and Immunity, University College London, London, United Kingdom.

https://doi.org/10.1016/j.vaccine.2019.09.004
0264-410X/

which is expressed on the surface of intestinal epithelial cells. Activation of the GC-C receptor triggers a signalling cascade which ultimately causes diarrhoea through the release of electrolytes and water into the gut lumen [14,15]. The ST peptides have three conserved disulfide bridges which are crucial for structural integrity and toxicity [12]. Three key challenges must be solved to succeed in making safe ST-based vaccines [12,16]. Firstly, STs are non-immunogenic due to their small size, and they must therefore be made immunogenic by coupling to an immunogenic carrier. Secondly, STs are potent toxins and must be made non-toxic. Finally, STs are similar to the endogenous GC-C receptor peptides guanylin and uroguanylin both in sequence and structure, and ST epitopes that induce unwanted immunological cross-reactions to these two ligands must, therefore, be altered [12,17–19]. To identify STh mutants with reduced or abolished toxicity, but with retained antigenicity allowing recognition by neutralizing anti-ST antibodies, we recently screened a library of all possible 361 single-amino acid STh mutants [18]. This screening led to the identification of our current lead ST toxoid candidate STh-A14T which has >800-fold lower toxicity than native STh, but which retains most epitopes that are needed to effectively induce a neutralizing anti-ST immune response [20].

Previously, ST has been rendered immunogenic mainly through coupling to protein carriers [12], but also through polymerization [21] and by coupling to T-helper cell epitopes bound to lipopeptide adjuvants [22]. An alternative and promising way of rendering small peptides immunogenic is to couple them to virus-like particles (VLPs) which are self-assembled viral envelope or capsid proteins [23,24]. Antigens can be presented on the VLP surface by the means of genetic fusions, enzymatic linkage, or chemical conjugation [24]. VLPs have ordered surfaces which allows for high density presentation of single, multivalent, or combinatorial antigens [25–28] and this orderly presentation of vaccine epitopes leads to more defined interactions with the immune system compared to when they are conjugated to the surface of regular single-protein carriers [29].

VLPs are also promising in terms of yielding highly stable and efficient vaccines [30]. VLP-based vaccines targeting Hepatitis B (HBV), Hepatitis E (HBE), and human papilloma virus (HPV) have already been approved for human use [31]. A large number of VLP-based vaccines are also being developed for bacterial and viral diseases, where the VLPs are either derived from the pathogens they are intended to protect against or they are used as carriers for presenting heterologous antigens [29,32,33]. A simple system that allows for spontaneous and irreversible *in vitro* conjugation of heterologous antigens to VLP surfaces has recently been described [34–36]. In this system, conjugation is facilitated by an isopeptide bond formed between an aspartic acid in the SpyTag polypeptide and a lysine in the SpyCatcher domain [34]. The SpyCatcher/Tag system has been used, in different configurations, to display malaria antigens on the Acinetobacter phage AP205 VLP surface [35,36].

In this study, we investigated the suitability of using the SpyCatcher-AP205 VLP system to render STh immunogenic, assessed the ability of the non-toxic STh-A14T mutant to elicit STh-neutralizing antibodies in mice, and we investigated the degree of cross-reactivity the serum antibodies had towards STp, guanylin, and uroguanylin.

2. Materials and methods

2.1. Cloning, expression, and purification of SpyTag-STh fusion peptides

To facilitate coupling to SpyCatcher-AP205 VLPs, we genetically fused the SpyTag to the N-terminus of native STh and STh-A14T, separated by a linker (Fig. 1A). The previously described pET-DsbC-STh and pET-DsbC-STh-A14T expression vectors [20] were used as backbones, and the insertions were accomplished using the Q5® Site-Directed Mutagenesis Kit (New England Biolabs, Ipswich, MA, USA), and the primers SpyT_lnk_STh_F: 5′-caaatgggg cagtggtggttcaggggttccggtAATAGTAGCAATTACTGCTG-3′ and SpyT_lnk_STh_R: 5′-gtcggcttgtaagcgtccaccattacaatgtgagcCTGAAAA TAAAGATTCTCGC-3′. The bases encoding the SpyTag and linker are shown in lower case, while the upper-case bases match the vectors. The first residue of the SpyTag was positioned immediately downstream of a Tobacco Etch Virus protease (TEV) cleavage sequence, thus exploiting TEV's flexibility in the P'1 position, allowing enzymatic release of SpyTag-ST fusion peptides no extra amino acids [37]. The resulting expression vectors, pET-DsbC-SpyT-STh and pET-DsbC-SpyT-A14T, were verified by sequencing.

The SpyTag-STh and SpyTag-STh-A14T fusion peptides, named SpyT-STh and SpyT-A14T, were produced by adapting our previously described system for expressing and purifying native ST and ST mutants [20]. In brief, chemically competent *E. coli* BL21 Star™ (DE3) (Invitrogen, Waltham, MA, USA) were transformed with pET-DsbC-SpyT-STh or pET-DsbC-SpyT-A14T, plated on LB-Agar supplemented with 50 μg/mL kanamycin, followed by incubation at 37 °C overnight. Single colonies were used to inoculate 5 mL Luria-Bertani (LB) growth medium supplemented with 50 μg/mL kanamycin, and incubated overnight at 37 °C and 200 rpm using a 25 mm throw. One mL overnight culture was used to inoculate 1 L Yeast Extract Tryptone (2X YT) broth supplemented with 2% glucose (w/v) and 50 μg/mL kanamycin. The culture was grown at 37 °C and 200 rpm using a 25 mm throw. When the optical cell density reached 0.6 at 600 nm the protein expression was induced by adding IPTG to a final concentration of 500 μM and the temperature was lowered to 18 °C before overnight expression.

Cells were harvested by centrifugation at 8,000 × g for 20 min followed by re-suspension in 10 mL lysis buffer (50 mM Tris-HCl, 300 mM NaCl, 20 mM Imidazole, 0.2% Triton X-100, 1 mg/mL lysozyme [pH 8]) per gram wet weight pellet. After 30 min incubation on ice, the bacteria were sonicated using an Ultrasonic homogenizer (Cole-Parmer Instrument Co., Vernon Hills, IL, USA) followed by clarification of the lysate at 20,000 × g for 20 min.

The lysate was loaded onto 5 mL HisTrap FF Crude Ni-NTA columns (GE Healthcare Life Sciences, Chicago, IL, USA) connected to an ÄKTA pure system (GE Healthcare Life Sciences). The bound peptides were washed in buffer A (50 mM Tris-HCl, 300 mM NaCl, 20 mM Imidazole [pH 8]) followed by elution in buffer B (50 mM Tris-HCl, 300 mM NaCl, 500 mM Imidazole [pH 8]). To cleave off the SpyT-tagged STs, we first performed a buffer exchange to TEV cleavage buffer (20 mM NaPi, 125 mM NaCl [pH 7.4]) using PD-10 desalting columns (GE Healthcare Life Sciences). To allow for TEV cleavage under non-reducing conditions, [38] glutathione (GSH) and glutathione disulfide (GSSG) (Sigma-Aldrich, St. Louis, MO, USA) was supplemented to final concentrations of 0.6 mM and 0.4 mM, respectively, after the buffer exchange.

After adding 1:30 M ratio of His-tagged TEV protease and incubating overnight at room temperature, the solution was passed a second time over a Ni-NTA agarose resin gravity column (Qiagen, Hilden, Germany) to bind and remove DsbC, uncleaved fusion protein and TEV. The flow through was collected and concentrated using 3 kDa cut-off Amicon™ Ultra-15 centrifuge filters (Merck Millipore, Burlington, MA, USA) before being loading onto a Superdex 30 PG HiLoad 16/600 size exclusion column (GE healthcare life sciences), operated by an ÄKTA pure system. Purified SpyT-STh and SpyT-A14T were eluted in phosphate buffer saline (PBS; 1.8 mM KH_2PO_4, 10 mM Na_2HPO_4, 2.7 mM KCl, 137 mM NaCl [pH 7.4]) followed by peptide concentration by using 3 kDa cut-off Amicon™ Ultra-15 centrifuge filters. The purified proteins were analysed on both SDS-PAGE (4–20% Mini-PROTEAN® TGX™ Precast Protein Gels (Bio-Rad, Hercules, CA, USA) and by MALDI-TOF/TOF mass

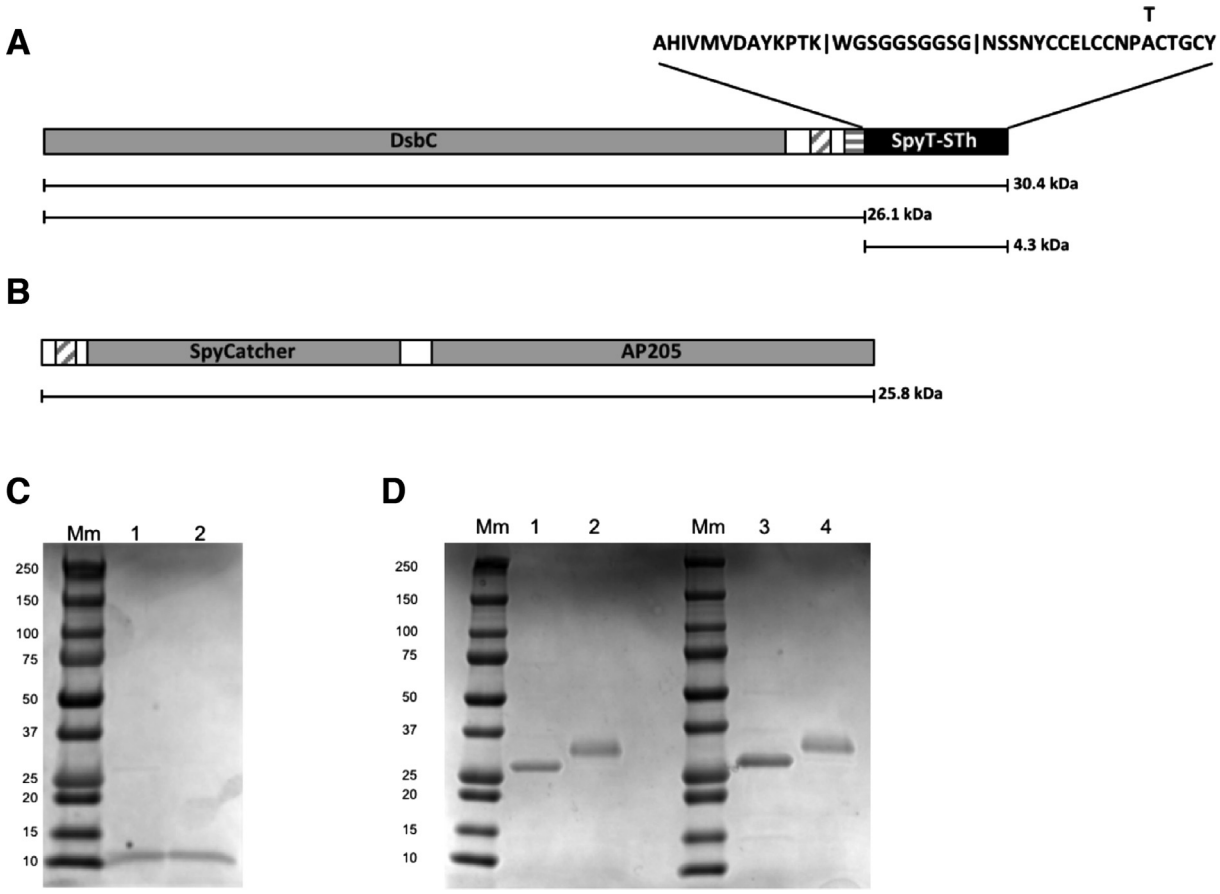

Fig. 1. Design and production of SpyT-STh, SpyT-A14T, AP205-SpyC, and the AP205-SpyC:SpyT-STh and AP205-SpyC:SpyT-A14T immunogens. (A) Illustration of the DsbC-His-TEV-SpyT-STh fusion protein. Linker sequences are shown in white, while His-tags and TEV cleavage sites are shown as cross- and horizontal-hatched regions, respectively. The sizes and molecular masses of the full-length fusion protein and the retrieved products after TEV protease cleavage are indicated with horizontal bars. The amino acid sequence of the SpyTag-linker-STh fusion protein is also shown, and the separations of the three regions are indicated by vertical lines, together with a 'T' which indicates the position of the A14T mutation. (B) Illustration of the AP205-SpyC fusion protein. The linker and His-tag are shown as white and cross-hatched regions, respectively. (C) SDS-PAGE gel showing purified SpyT-STh (lane 1), purified SpyT-A14T (lane 2), and a molecular marker (Mm). (D) SDS-PAGE gel showing purified AP205-SpyC proteins (lanes 1 and 3), purified AP205-SpyC:SpyT-STh conjugates (lane 2), purified AP205-SpyC:SpyT-A14T (lane 4) conjugates, and a molecular marker (Mm).

spectrometry by using an ULTRAFLEX II (Bruker Daltonics, Bremen, Germany) as previously described [20].

2.2. Antigenicity of purified SpyT-STh and SpyT-A14T

The antigenicities of SpyT-STh and SpyT-A14T were analysed in both a monoclonal and a polyclonal competitive ELISA as described previously [17]. In brief, the ELISAs were performed by coating the wells of Nunc Immobilizer Amino Plates (Thermo Fisher Scientific, Waltham, MA, USA) with 0.11 μg STh-ovalbumin conjugates in 100 μL ELISA PBS buffer (3.25 mM Na_2HPO_4, 9.6 mM NaH_2PO_4, 146 mM NaCl [pH 7.4]) overnight at 4 °C. The wells were then emptied and blocked by adding 180 μL ELISA PBS-T (3.25 mM Na_2HPO_4, 9.6 mM NaH_2PO_4, 146 mM NaCl, 0.05% (v/v) Tween-20, [pH 7.4]) containing 1% (w/v) ovalbumin and incubated for 1 h at room temperature with gentle shaking. Following 3 washes with ELISA PBS-T, we added 60 μL SpyT-STh, SpyT-A14T, or native STh that had been diluted 12 times 3-fold from 10 μM in ELISA PBS-T. We then added 60 μL 1:15,000 diluted anti-STp C30 mAb (Clone M120530; Fitzgerald, North Acton, MA, USA), which is an ST-neutralizing mAb that recognizes an epitope centred around Y19 in native STh [18], or 60 μL 1:4,000 diluted ST-neutralizing polyclonal anti-STh antibody, which was kindly provided by John D. Clements at Tulane University, that has been generated by immunizing rabbits with a bovine serum albumin (BSA)-STh conjugate followed by Protein A purification of the resulting serum. After 2 h of incubation with gentle shaking at room temperature, we washed the plates 3 times with ELISA PBS-T before adding 100 μL 1:4000 diluted anti-mouse IgG antibody conjugated to alkaline phosphatase (Product code: ab6729, Abcam, Cambridge, United Kingdom). After 1 h incubation at room temperature and 3 subsequent washes with ELISA PBS-T, we added 100 μL developing reagent (250 mM diethanolamine, 0.5 mM $MgCl_2$, 0.5 mg/mL 4-Nitrophenyl phosphate disodium salt [pH 9.8]) and measured the absorbance at 405 nm at a time when the well with the strongest signal had an absorbance between 1.0 and 2.0 in a Hidex Sense microplate reader (Hidex, Turku, Finland).

2.3. AP205-SpyC expression, purification, and VLP production

The pKB_215 - 6xHIS-SpyCatcherΔN1-CP3 plasmid encoding the SpyCatcher coupled to the AP205 coat protein (AP205-SpyC) was a kind gift from Mark Howarth and Karl D. Brune, University of Oxford. The expression and purification of AP205-SpyC was performed as previously described [35], but with a few modifications. The plasmid was transformed into the chemically competent *E. coli* strain OverExpress™ C41(DE3) (Lucigen, Middleton, WI, USA) and plated on LB-Agar supplemented with 100 μg/mL ampicillin. Following overnight incubation at 37 °C, 4 individual colonies were added to 500 mL 2xYT broth containing 20 μg/mL ampicillin. After

overnight incubation at 37 °C and 50 rpm using a 25 mm throw, 500 mL fresh 2xYT broth, and fresh ampicillin to a final concentration of 20 μg/mL (assuming the previously added ampicillin had been degraded), was added before continuing the incubation at 100 rpm shaking. When the optical density at 600 nm reached 0.5–0.7 the temperature was reduced to 22 °C, and after 30 min IPTG was added to a final concentration of 500 μM for overnight expression at 200 rpm using a 25 mm throw.

Cells were harvested by centrifugation at 5500 × g for 15 min at 4 °C. For each litre culture, the obtained bacterial pellet was resuspended in 10 mL lysis buffer (20 mM Tris-HCl, 150 mM NaCl, 75 mM Imidazole, 0.1% Triton X-100, 0.1% Tween-20, 25 U/mL Benzonase Nuclease (Merck Millipore), 0.2 mg/mL lysozyme, 1x cOmplete™, EDTA-free Protease Inhibitor Cocktail (Roche, Mannheim, Germany) [pH 7.8]). Following 10 min incubation at room temperature, the resuspended cells were frozen at −80 °C for 30 min before thawing and sonication using an Ultrasonic homogenizer (Cole-Parmer Instrument Co.). The lysate was then cleared by centrifugation at 15,000 × g for 20 min at 4 °C, moving the supernatant to a fresh tube, repeating the centrifugation, and then passing the supernatant through a 0.4 μm Whatman™ Nucleopore Polycarbonate filter (GE Healthcare Life Sciences) and incubation in room temperature for 5 min after adding 250 U Benzonase Nuclease (Merck Millipore). For each litre initial culture, the lysate was mixed with 400 μL Ni-NTA agarose (Qiagen) that had been equilibrated with 20 mM Tris-HCl, 150 mM NaCl, 75 mM imidazole [pH 7.8]. After 10 min incubation at 4 °C, the Ni-NTA agarose containing the bound AP205-SpyC was transferred to a 10 mL Econo-Pac polypropylene column (Bio-Rad). The flow through was allowed to pass through the column, collected and loaded onto the column once more before washing the column with 3 column-volumes of Washing buffer (20 mM Tris-HCl, 150 mM NaCl, 100 mM imidazole [pH 7.8]) followed by elution using elution buffer (50 mM glycine, 25 mM sodium citrate, 2 M Imidazole, 0.1% (v/v) tween-20 [pH 8.5]). 1 mL fractions were collected and analysed by SDS-PAGE, and the fractions containing AP205-SpyC at high concentrations were pooled and dialyzed by using a 300 kDa cut-off membrane (Spectrum Laboratories, Rancho Dominguez, CA, USA) against Dialysis buffer (50 mM glycine, 25 mM sodium citrate, 0.1% (v/v) tween-20 [pH 8]). The A205-SpyC monomers self-assemble into VLPs and the dialysis allows for small non-VLP proteins to escape while the high molecular weight VLPs are retained.

2.4. AP205-SpyC:SpyT-ST VLP production

Conjugation of SpyT-STh and SpyT-A14T to the AP205-SpyC VLPs was achieved by simply mixing AP205-SpyC VLPs with SpyT-STh or SpyT-A14T in a 1:2 M ratio to assemble AP205-SpyC:SpyT-STh and AP205-SpyC:SpyT-A14T VLPs. The conjugation was performed overnight at room temperature in Dialysis buffer and conjugation was monitored by SDS-PAGE.

Following conjugation, unbound SpyT-STh or SpyT-A14T was removed by dialysis by using a 300 kDa cut-off membrane (Spectrum Laboratories), followed by centrifugation at 17,000 × g for 30 min at 4 °C to remove any protein aggregates. To remove any co-purified endotoxins, the conjugates were filtered through a 0.2 μm PTFE Whatman™ filter and endotoxins were removed by using a Triton X-114-based phase separation method as described previously [39]. The endotoxin levels of the cleaned VLP conjugates were below 1 endotoxin units (EU) per mL, as determined by using the Pierce™ LAL Chromogenic Endotoxin Quantitation Kit (Thermo Fisher Scientific). The VLP conjugates were then kept at 4 °C, and all subsequent procedures were performed by using endotoxin-free certified consumables. The ST-conjugated VLP capsid protein concentrations were measured by using the Pierce BCA Protein Assay Kit (Thermo Fisher Scientific) and subsequently diluted to 300 μg/mL in Endotoxin-free Dialysis buffer (50 mM glycine, 25 mM sodium citrate, 0.1% (v/v) Tween 20 [pH 8.0]).

2.5. Immunizations

Immunizations and serum collection were performed by GenScript (Piscataway, NJ, USA). Five age-matched, 9 week old, female BALB/C mice were immunized with AP205-SpyC:SpyT-STh, five were immunized with AP205-SpyC:SpyT-A14T, and five control mice were immunized with molar equivalents of unconjugated SpyT-STh. The mice received the primary immunization and booster immunizations on day 14 intramuscularly in the rear leg with 100 μL doses that contained the equivalent of 1 nmol (2 μg) ST peptide. This implies that estimated total immunogen doses of AP205-SpyC:SpyT-STh and AP205-SpyC:SpyT-A14T were 28 μg, and that of SpyT-STh was 4.3 μg. No adjuvants were used, pre-immunization sera were collected for all the mice, and the mice were sacrificed and sera were collected on day 28.

2.6. Estimation of endpoint serum antibody titers by ELISA

Serum samples from each immunized mouse were titrated for anti-STh and anti-AP205-SpyC IgG antibodies in ELISA assays. After coating the wells of Nunc Immobilizer Amino plates overnight with 40 ng native STh in 100 μL ELISA PBS buffer or 100 ng AP205-SpyC in 100 μL coating buffer (15 mM sodium carbonate, 35 mM sodium bicarbonate), we emptied the wells and added 120 μL mouse serum that had been serial diluted 2-fold from 1:1000 to 1:2,048,000 in ELISA PBS buffer. Following incubation for 1 h at room temperature, 3 washes with PBS-T, 1 h incubation with 100 μL anti-mouse IgG antibody conjugated to alkaline phosphatase (Abcam), and 3 washes with PBS-T, we added 100 μL Diethanolamine buffer and read the absorbance at 405 nm on a Hidex Sense microplate reader (Hidex). The titer was defined as the highest dilution that gave a signal over background ratio of ≥ 2.1.

2.7. Analysis of immunological cross-reactivity by competitive ELISA

To measure the reactivity between mouse serum antibodies and native STh, STp, guanylin, and uroguanylin, we used competitive ELISAs as described previously [17]. The competitive ELISAs were performed as described above, but with the following modifications. In these assays, we coated the plates with 4 ng native STh per well, and we used STh, STp, guanylin, and uroguanylin that had been diluted 3-fold 12 times from 10 μM to outcompete the mouse serum antibody binding to the immobilized STh. Each serum sample was analysed three times in independent experiments.

2.8. T84 cell toxicity assay

The T84 cell toxicity assay was performed as described previously [17]. Briefly, T84 cells (ATCC, Rockville, MD, USA) were seeded and grown to confluence in Nunc 24-well plates (Thermo Fisher Scientific) containing Gibco™ Dulbecco's Modified Eagle Medium/Nutrient Mixture F-12 (DMEM/F-12; Thermo Fisher Scientific) supplemented with 10% foetal bovine serum (Sigma-Aldrich) and 0.2% gentamicin (LONZA, Basel, Switzerland). Cells were washed thrice with 500 μL DMEM/F-12 and incubated with 200 μL DMEM/F-12 containing 1 mM 3-isobutyl-1-methylxanthine (Sigma-Aldrich) for 10 min at 37 °C in 5% CO_2. The toxicity assays were performed in three independent experiments. The peptides to be tested were first serially diluted, 5 times 2-fold from 1 μM, in 200 μL DMEM/F-12 medium before being

added to individual wells. After incubating for 60 min at 37 °C in 5% CO_2, the medium was aspirated and cells were lysed by adding 500 μL 0.1 M HCl and incubated at 20 °C for 20 min. The lysates were then cleared by centrifugation at 16,000 × g for 10 min and cGMP levels in the resulting supernatants were determined using a cGMP enzyme immunoassay kit (Enzo Life Sciences Inc., Farmingdale, NY, USA) according to the manufacturer's instructions.

2.9. T84 cell neutralization assay

To measure to what extent the mouse serum antibodies could neutralize the toxic activity of native STh, we diluted the serum to 1:5, 1:10, 1:100, and 1:1000 in DMEM/F-12 medium, added native STh to 40 nM, and incubated the solutions overnight at 4 °C. The samples were then tested in the T84 cell assay as described above. These analyses were repeated in three independent experiments.

2.10. Data and statistical analyses

GraphPad Prism 8 (GraphPad Software, La Jolla, CA) was used for plots and regression analyses. Analyses of competitive ELISAs using four-parameter log-logistic regression were performed as previously described [19], using the following constraints: the bottom parameter was a shared value for all data sets, and the top parameter was set to a maximum value of 100. To test whether differences between the 50 percent inhibitory concentration (IC_{50}) mean values of SpyT-STh and SpyT-A14T were statistically different to that of the control STh, we used ordinary one-way analysis of variance (ANOVA), and corrected for multiple testing using Dunnet's test. Cross-reacting fractions were calculated for STp, uroguanylin, and guanylin, also as previously described [19]. Briefly, using the same constraints as above, four-parameter log-logistic regression models were generated using the R statistical computing environment and the drc R package [19,40]. The fitted models were used to calculate the 90 percent inhibitory concentrations (IC_{90}) for STh, which were used to calculate the percent inhibition of binding for each of the other peptides at the IC_{90} of STh. The estimated values were adjusted by subtracting the bottom parameter estimate, and cross-reacting fractions were calculated by dividing the adjusted percent inhibition value of each peptide by the corresponding inhibition values for STh.

3. Results and discussion

3.1. Expression and purification of STh and STh-A14T genetically fused to SpyTag

To investigate the potential of VLPs for making ST immunogenic, we chose to use the newly developed AP205 VLP system, where the AP205 protein has been genetically fused to a SpyCatcher domain [35]. A prerequisite for coupling heterologous proteins to AP205 using this system is to genetically fuse the desired protein to a SpyTag peptide. Hence, we fused both native STh and STh-A14T to the C-terminus of the SpyTag, separated by a spacer (Fig. 1A). The two fusion peptides were named SpyT-STh and SpyT-A14T, respectively. To express the fusion peptides in *E. coli*, we adopted our previously published recombinant ST purification system [20]. The SpyT-STh and SpyT-A14T peptides were genetically fused to the C-terminus of the disulfide isomerase DsbC linked by a His-tag for purification and a TEV protease cleavage site for the release of free fusion peptide (Fig. 1A). DsbC assists in the formation of the three disulfide bridges of ST, which is necessary for correct folding. After purification SpyT-STh and SpyT-A14T peptides were concentrated and analysed by SDS-PAGE (Fig. 1C). Although SDS-PAGE analyses of the purified SpyT-STh and SpyT-A14T peptides indicated sizes > 4.3 kDa (Fig. 1C), an immunoblot using the C30 mAb confirmed that the band on the gel contained ST (not shown). Moreover, mass spectrometry analysis confirmed that the purified peptides indeed were SpyT-STh and SpyT-A14T. Assuming both peptides have 6 oxidized cysteines, representing 3 disulfide bonds, the theoretical monoisotopic masses for the SpyT-STh and SpyT-A14T are 4284.74 and 4314.75 Da, respectively. We measured the peptides to be 4284.75 Da and 4315.09 Da, respectively. This indicates that the purified peptides had intact disulfide bridges, which is a requirement for correct folding.

3.2. Biological activity and antigenicity of SpyT-STh and SpyT-A14T

Coupling ST to a protein carrier by chemical conjugation has been reported to significantly reduce its toxicity [41]. To assess the impact of the SpyTag and linker peptide on the biological activity of STh, we compared the toxicity of SpyT-STh and SpyT-A14T with that of native STh in the T84 cell assay (Fig. 2A). SpyT-STh had somewhat lower toxicity than native STh, whereas SpyT-A14T which is based on the STh-A14T mutant with >800-fold reduced toxicity [20], had no detectable toxicity. The reduced toxicity of SpyT-STh may be attributed to steric hindrance by the fused SpyTag and linker peptides and/or to the presence of SpyT-STh isomers with alternative disulfide bridge configurations [20].

The structure of ST variants made immunogenic through genetic fusions or chemical conjugations should be as close as possible to that of native ST, to ensure that protective epitopes are intact and to maximize the likelihood of eliciting antibodies that neutralize native ST. We used the neutralizing C30 monoclonal anti-STp antibody that recognizes an epitope centered around Y19 [18], and a neutralizing polyclonal anti-STh antibody to compare the epitope repertoire of SpyT-STh and SpyT-A14T with that of native STh in competitive ELISAs. The abilities of SpyT-STh and SpyT-A14T to inhibit the monoclonal antibody binding to immobilized native STh was 4.2-fold (mean difference −13 nM, P = 0.0001) and 2.3-fold (mean difference −5 nM, P = 0.0001) lower than that of native STh (Fig. 2B). SpyT-STh and SpyT-A14T also had 5.0-fold (mean difference −12 nM, P = 0.001) and 1.3-fold (mean difference −0.8 nM, P = 0.6) reduced ability, respectively, to inhibit binding of the polyclonal antibody (Fig. 2C). We cannot rule out partial masking of epitopes by the SpyTag, but overall, the results suggest that the epitope repertoires of SpyT-STh and SpyT-A14T are largely shared with that of STh.

3.3. Conjugation of SpyT-STh and SpyT-A14T to AP205-SpyC

The AP205-SpyC VLP scaffold (Fig. 1B) was expressed and purified as previously described [35]. The A205-SpyC monomers self-assemble into VLPs, and extensive dialysis using a 300 kDa cutoff membrane allows small non-VLP proteins to escape while retaining the high molecular weight VLPs. SDS-PAGE analysis of the AP205-SpyC VLPs displayed only one visible band, migrating close to the expected molecular monomer mass of 25.8 kDa, suggesting high purity (Fig. 1D).

To prepare the immunogens, AP205-SpyC was mixed separately with SpyT-STh or SpyT-A14T at 1:2 M ratios, and unbound peptides were removed by dialysis using a 300 kDa cutoff membrane. SDS-PAGE analysis revealed only one band for each of the conjugates, migrating close to the expected molecular mass of 29.1 kDa (Fig. 1D). This suggest that the spontaneous isopeptide bond conjugation reaction was efficient, and that the resulting VLPs have hapten-carrier ratios that approach the theoretical number of 180 haptens per particle. The VLP conjugates were named AP205-SpyC:SpyT-STh and AP205-SpyC:SpyT-A14T.

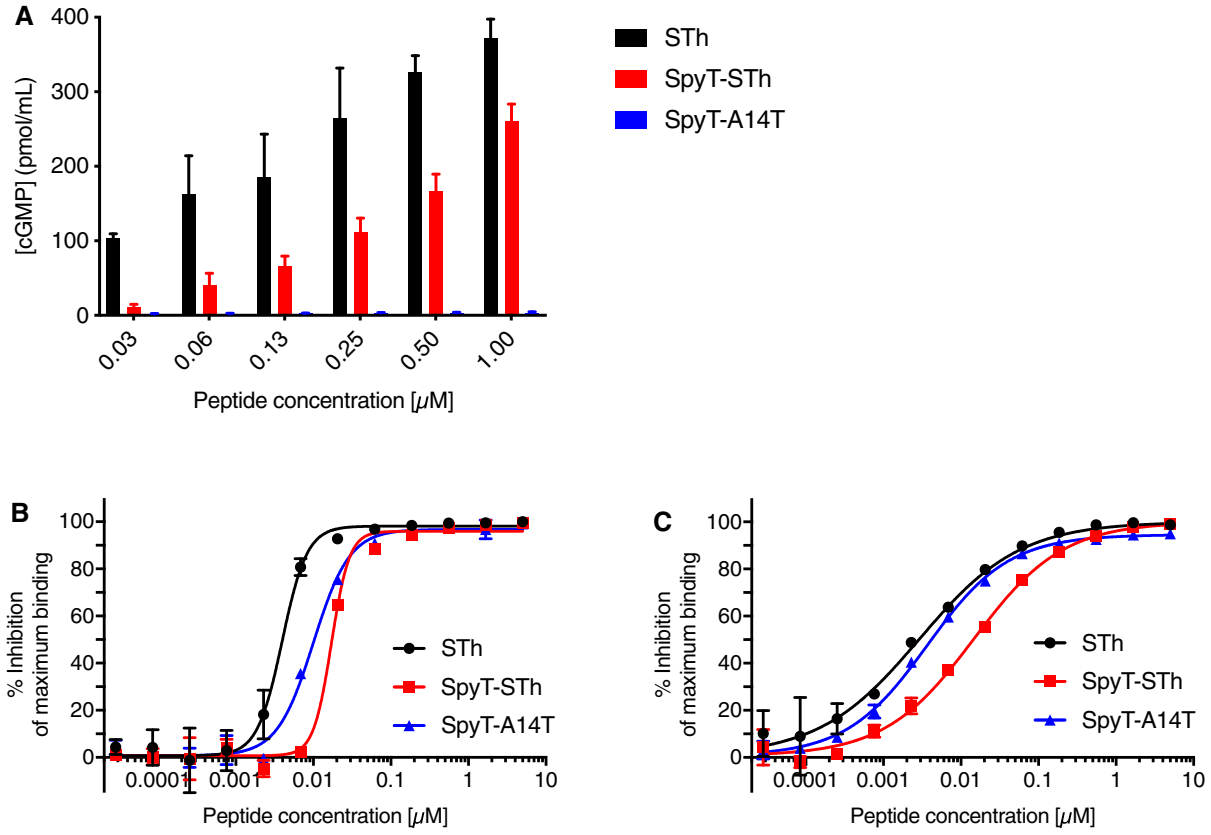

Fig. 2. Toxicity and antigenicity of SpyT-STh and SpyT-A14T (A) T84 cell toxicity assays, where a dilution series of equimolar amounts of SpyT-STh (red), SpyT-A14T (blue) and native STh (black) were tested for the ability to induce cellular cGMP. The error bars indicate the standard deviations from three independent experiments. Note that SpyT-A14T did not induce any noticeable cGMP production and its values are therefore, not clearly visible. (B) and (C) show results from the antigenicity testing of SpyT-STh and SpyT-A14T. Competitive ELISAs were used to investigate the ability of equimolar amounts of SpyT-STh (red), SpyT-A14T (blue), and native STh (black) to outcompete binding of (B) the anti-STp monoclonal antibody C30 and (C) a polyclonal anti-STh antibody to immobilized STh. Each data point represents the mean from three independent assays, and the error bars, representing standard deviations, are shown where they exceed the size of the data point symbol. (For interpretation of the references to colour in this figure legend, the reader is referred to the web version of this article.)

3.4. Immunization of mice and serum antibody titers

We immunized five mice each with AP205-SpyC:SpyT-STh and AP205-SpyC:SpyT-A14T VLPs, as well as five mice with the SpyT-STh peptide alone as a control. The pre-immune sera from all mice used in the immunizations, as well as the endpoint sera for the mice immunized with SpyT-STh alone, had no detectable anti-STh or anti-AP205-SpyC serum IgG antibodies, at the highest concentration tested which was a 1:1000 dilution of the sera. The lack of an anti-STh immune response from the mice immunized with SpyT-STh suggest that the SpyT-STh itself is not immunogenic. The endpoint sera from the mice immunized with AP205-SpyC:SpyT-STh and AP205-SpyC:SpyT-A14T all displayed high titers, ranging from 4000 to 32,000 for anti-STh (Fig. 3A) and 64,000 to 512,000 for anti-AP205-SpyC (Fig. 3B). Interestingly, the mean anti-ST titers of sera from mice vaccinated with AP205-SpyC:SpyT-STh (mean titer: 18,400) were similar to those from mice vaccinated with AP205-SpyC:SpyT-A14T (mean titer: 16,000), indicating that the A14T mutation does not have a major negative impact on the quality of the anti-STh immune response, which makes STh-A14T a promising antigen for use in ST-based vaccines.

3.5. Serum antibody STh-neutralization

To assess whether the serum antibodies from mice immunized with AP205-SpyC:SpyT-STh and AP205-SpyC:SpyT-A14T are able to neutralize the toxic activity of native STh, we tested the sera in T84 cell neutralization assays. When diluted 1:5, sera from both groups of mice almost completely inhibited STh-induced cGMP production, suggesting the sera contained antibodies that effectively neutralize STh (Fig. 4). Diluting the sera 1:10 and 1:100-fold gave only partial neutralization, and no or very little neutralization could be seen when diluting the sera 1:1000. Interestingly, there appeared to be very little variation in these neutralization estimates, both within and between groups. This is in contrast to a study of STh- and STp-bovine serum albumin conjugates, where the ST-neutralizing immune responses varied both between and within immunization groups [19]. Although further studies are needed to identify the underlying cause of the lower variability, we suspect the homogeneous and orderly presentation of STs on the surface of the VLPs, in addition to the omission of additional adjuvants result in a more predictable immune response than more traditional formulations. In addition, the finding that the STh neutralization abilities of sera from mice immunized with the STh-A14T antigens appeared to match those from mice immunized with native STh antigens suggest that the A14T mutation does not impair the ability to elicit STh-neutralizing antibodies.

3.6. Immunological cross-reactivity

STh and STp are very similar both in sequence and structure: their sequences are 78% identical, and 4 of the 5 amino acid differences are found in the N-terminus [12]. This implies that the two peptides share relevant epitopes, and that immune responses

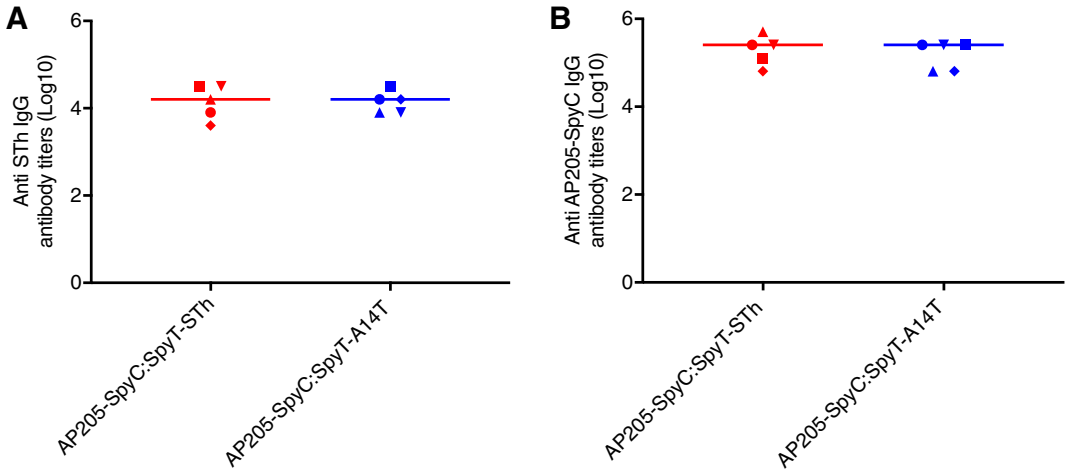

Fig. 3. Endpoint serum antibody titers. The endpoint sera from ten mice were titrated in ELISAs where STh (A) or AP205-SpyC (B) was immobilized on ELISA plates and an anti-mouse IgG antibody was used to detect bound anti-STh and anti-AP205-SpyC antibodies from five mice immunized with AP205-SpyC:SpyT-STh (in red) and five mice immunized with AP205-SpyC:SpyT-A14T (in blue). The titers were defined as the highest dilutions that had signal over background ratios of ≥ 2.1. Each data point represents the mean antibody titer from three independent ELISAs, and the horizontal lines represent the mean of these titers from all five mice. (For interpretation of the references to colour in this figure legend, the reader is referred to the web version of this article.)

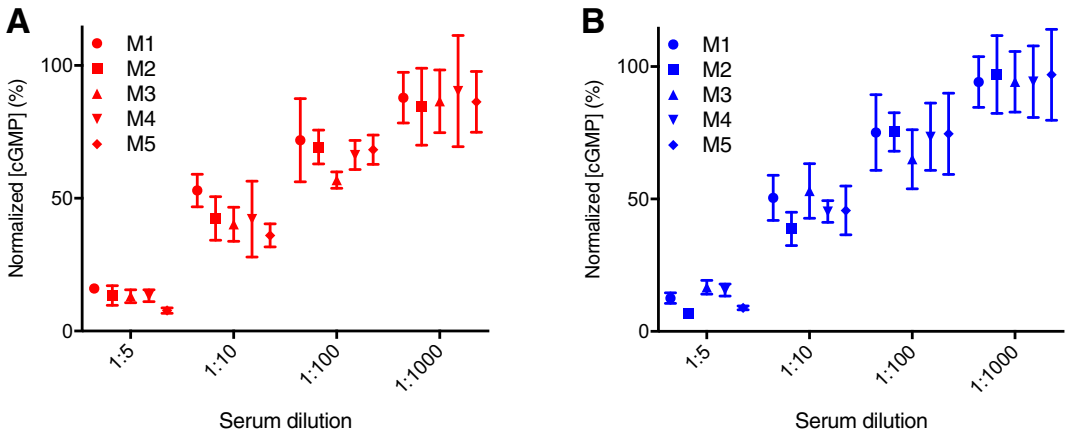

Fig. 4. Serum STh neutralization. Dilutions of endpoint sera were tested for their ability to neutralize native STh in T84 cell neutralization assays. The data points represent the mean result from three independent experiments with sera from 5 mice (M1 to M5) immunized with (A) AP205-SpyC:SpyT-STh (in red) or with (B) AP205-SpyC:SpyT-A14T (in blue). The error bars, which indicate the standard deviation based on results from three independent experiments, are shown where they exceed the size of the data point symbols. (For interpretation of the references to colour in this figure legend, the reader is referred to the web version of this article.)

induced by STh-based vaccines can be expected to cross-react with STp and offer protection against STp-producing ETEC strains. The endogenous GC-C receptor activating peptides, uroguanylin and guanylin, are also similar to the ST toxins, with 69% and 53% sequence identity to STh, respectively [12]. Potential interference with the natural regulation of the GC-C receptors could occur if an ST-based vaccine elicits antibodies that cross-react strongly with guanylin or uroguanylin. To study both wanted (STp) and unwanted (uroguanylin and guanylin) immunological cross-reactions from immunizations with STh-based antigens, we performed competitive ELISAs where we tested the ability of native STh, STp, guanylin and uroguanylin to compete with the coated STh for binding to the antibodies present in the mouse sera (Fig. 5). As expected, STh completely outcompeted binding of anti-STh antibodies to the STh coating at the highest concentrations, and STp was almost as efficient in doing so, suggesting strong cross-reaction to STp (Fig. 5A). The same pattern was also observed with the anti-STh-A14T antibodies (Fig. 5B). In contrast, for all sera tested, there seemed to be low levels of antibodies cross-reacting with uroguanylin and guanylin (Fig. 5A and B).

For consistent comparisons of immunological cross-reactivity between sera, we used the 90 percent inhibitory concentration (IC_{90}) of STh as a common reference point (Fig. 5A and B). For each peptide, the cross-reacting fraction of antibodies was calculated by dividing the percent inhibition of each peptide at the reference concentration with that of STh (Fig. 5C). For the anti-STh sera, the median cross-reacting fraction for STp was 0.87 (range 0.67–0.93), and for the anti-STh-A14T sera, it was 0.76 (range 0.68–0.81). For uroguanylin, the median cross-reacting fractions were 0.10 (range 0.2–0.11) and 0.12 (range 0.8–0.15), respectively, and for guanylin they were 0.08 (range 0.4–0.11) and 0.06 (range 0.05–0.12), respectively. This contrasts to what was previously observed in serum samples from mice that had been subcutaneously immunized with adjuvanted solutions of STh- and STp-bovine serum albumin conjugates [19]. In that study, much higher levels of cross-reacting antibodies to both uroguanylin and guanylin were observed in individual mice, with maximum cross-reacting fractions of 0.55 and 0.42, respectively. The difference in cross-reacting immune responses between the two studies could be an effect of differences in antigen presentation, route of

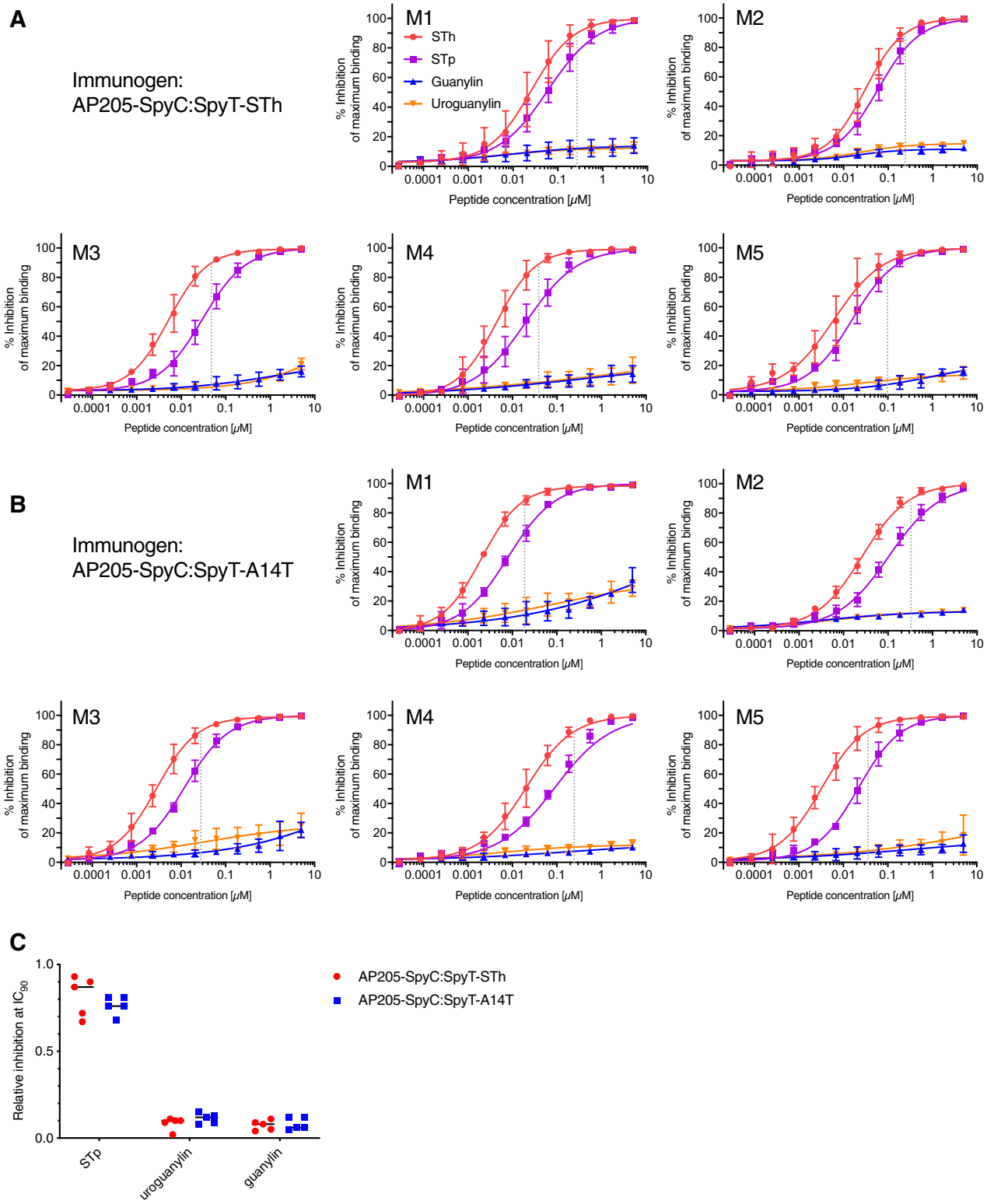

Fig. 5. Immunological cross-reactivity. (A) Cross-reactivity of sera from the five mice immunized with AP205-SpyC:SpyT-STh (one graph per mouse, labelled M1 to M5). The sera were mixed with STh (red), STp (purple), guanylin (blue), or uroguanylin (orange) in a competitive ELISA to evaluate to what extent these peptides could outcompete binding of serum antibodies to immobilized STh. Each data point represents the mean of three independent experiments, the error bars, which are shown where they exceed the size of the data point symbol, represent the standard deviations, and the graph lines are regression curves generated by four-parameter logistic regression analyses. Peptide concentrations are plotted on a logarithmic scale on the horizontal axis, and the vertical axis shows percent inhibition, which is given as a percentage of the maximum binding of the serum antibodies measured in the absence of a competing peptide. The dotted line represents the 90 percent inhibitory concentration (IC_{90}) of STh. (B) Cross-reactivity of sera from the five mice immunized with AP205-SpyC:SpyT-A14T (one panel per mouse, labelled M1 to M5). The assay and analysis were performed as in (A). (C) Assessment of cross-reactive fractions at IC_{90} of STh. For each serum, four-parameter logistic regression was performed, and the IC_{90} concentrations were calculated for STh, and were used to calculate the cross-reacting fractions for each peptide relative to that of STh. The plot shows the inhibition relative to that of STh at IC_{90} for STh (vertical axis) for each peptide (horizontal axis) in each serum (anti-AP205-SpyC:SpyT-STh in red, anti-AP205-SpyC:SpyT-A14T in blue), and the lines depict median cross-reactive fractions. (For interpretation of the references to colour in this figure legend, the reader is referred to the web version of this article.)

immunization, and/or the use of Freund's adjuvant. The low level of unwanted immunological cross-reactions observed in this study is encouraging for the prospects of developing a safe ST-based vaccine.

4. Conclusions

VLPs are known to be highly immunogenic and are increasingly being explored for use as carriers for presenting heterologous antigens [25–28]. Here, we have for the first time used VLPs to make both native STh and the non-toxic mutant STh-A14T immunogenic. We have shown that immunizing with the AP205-SpyC:SpyT-STh and AP205-SpyC:SpyT-A14T VLPs consistently elicited anti-STh antibody responses in mice, that the resulting antibodies were able to neutralize STh and STp, and that the immunization produced little or no unwanted immunological cross-reaction to uroguanylin and guanylin. This is also the first time immunizations with ST antigens have given anti-ST immune responses without the use of adjuvants. Although further studies are needed, we suspect the improved quality of the anti-ST immune responses may partially be a result of omitting Freund's complete and incomplete adjuvant from the vaccine formulations. In addition, the well-defined nature of VLPs allows for heterologous antigens to be presented in a highly ordered manner, which may have resulted in better inter-individual and inter-group immune response consistencies both in terms of antibody titer, the ability to neutralize native STh, and in fewer and lower levels of unwanted cross-reactive immune responses.

These encouraging results warrant further experiments. To ensure consistent immune responses also in future experiments, one must ensure that the STh-A14T-coupled AP205 VLPs forms stable particles of uniform size. This can be addressed using methods such as electron microscopy and dynamic light-scatting analysis. In addition, antigenicity studies using monoclonal antibodies with known epitopes can be performed to identify exposed, and possibly cross-reacting, epitopes [19]. In this first study using VLPs to make native STh and the toxoid STh-A14T immunogenic, we immunized mice intramuscularly and characterized serum IgG responses. Protection against the ST toxin *in vivo* will require a good mucosal immune response, and hence, future studies should be expanded to also characterize faecal IgA antibody responses. To ensure a good mucosal immune response, oral delivery of an ST vaccine is a natural first choice. However, it has recently been shown that the non-toxic double-mutant LT (dmLT), which is a potent adjuvant, has the potential to elicit pathogen-specific immunity in the intestinal tract with non-mucosal immunization [42]. This is a highly attractive alternative for an ST vaccine for two reasons. First, parenteral immunizations require substantially less material than oral immunizations and parenteral vaccines seem to be less prone to vaccine underperformance associated with environmental enteropathy than oral vaccines [43]. Second, administering an ST vaccine with dmLT as an adjuvant has the potential of eliciting a complete anti-toxin immune response that can protect against both ST and LT. It will be important to assess whether the addition of an adjuvant, such as dmLT, to an ST-VLP vaccine leads to increased immunological cross-reactivity towards uroguanylin and guanylin. The importance of this is underscored by the implication of these endogenous ligands in several diseases and biological processes, including inflammatory bowel disease, ulcerative colitis, colonic hypersensitivity, appetite regulation, and attention deficit hyperactivity [19].

In conclusion, the results generated in this study suggest that using VLPs is an attractive approach for making safe and effective ST-based vaccines. Moreover, the results strongly suggest that the mutant variant STh-A14T is an excellent candidate for an ETEC vaccine component.

Author contributions

Morten L. Govasli conceived and designed the experiments; Morten L. Govasli and Yuleima Diaz performed the experiments; Morten L. Govasli, Pål Puntervoll, and Yuleima Diaz analysed the data; All authors contributed to the writing of the paper. All authors accepted the final version of the paper.

Declaration of Competing Interest

The authors declare that they have no known competing financial interests or personal relationships that could have appeared to influence the work reported in this paper.

Acknowledgements

We thank Dr. Mark Howarth and Dr. Karl D. Brune for providing the plasmid encoding AP205-SpyC as well as for scientific discussion regarding the VLP platform. Synthetic STh was a kind gift from Dr. Yves-Marie Coic and Dr. Laurence Mulard, Institute Pasteur, Paris, France. The MALDI-MS analysis was performed at the Proteomics core facility, Department of Biosciences, University of Oslo, Norway. We thank Dr. Ephrem Debebe Zegeye, Dr. Hans Steinsland, Dr. Halvor Sommerfelt, Dr. Øyvind Halskau, Dr. Øyvind Strømland for reviewing the manuscript. The research leading to these results was supported by the Research Council of Norway through the Global Health and Vaccination Research Programme (GLOBVAC) [grant number 234364], by PATH, USA [grant number 102290-002], and by The Meltzer Research Fund, Norway [grant to Govasli].

References

[1] Fischer Walker CL, Perin J, Aryee MJ, Boschi-Pinto C, Black RE. Diarrhea incidence in low- and middle-income countries in 1990 and 2010: a systematic review. BMC Public Health 2012;12:220. https://doi.org/10.1186/1471-2458-12-220.

[2] Walker CLF, Rudan I, Liu L, Nair H, Theodoratou E, Bhutta ZA, et al. Global burden of childhood pneumonia and diarrhoea. Lancet (London, England) 2013;381:1405–16. https://doi.org/10.1016/S0140-6736(13)60222-6.

[3] GBD 2015 Mortality and Causes of Death Collaborators. Global, regional, and national life expectancy, all-cause mortality, and cause-specific mortality for 249 causes of death, 1980–2015: a systematic analysis for the Global Burden of Disease Study 2015. Lancet (London, England) 2016; 388: pp. 1459–544. doi: https://doi.org//10.1016/S0140-6736(16)31012–1.

[4] Liu J, Platts-Mills JA, Juma J, Kabir F, Nkeze J, Okoi C, et al. Use of quantitative molecular diagnostic methods to identify causes of diarrhoea in children: a reanalysis of the GEMS case-control study. Lancet 2016;388:1291–301. https://doi.org/10.1016/S0140-6736(16)31529-X.

[5] Platts-Mills JA, Babji S, Bodhidatta L, Gratz J, Haque R, Havt A, et al. Pathogen-specific burdens of community diarrhoea in developing countries: a multisite birth cohort study (MAL-ED). Lancet Glob Heal 2015;3. https://doi.org/10.1016/S2214-109X(15)00151–5.

[6] Diemert DJ. Prevention and self-treatment of traveler's diarrhea. Clin Microbiol Rev 2006;19:583–94. https://doi.org/10.1128/CMR.00052-05.

[7] Qadri F, Saha A, Ahmed T, Al Tarique A, Begum YA, Svennerholm A-M. Disease burden due to enterotoxigenic *Escherichia coli* in the first 2 years of life in an urban community in Bangladesh. Infect Immun 2007;75:3961–8. https://doi.org/10.1128/IAI.00459-07.

[8] PATH, BIO ventures for Global Health. The Case for Investment in Enterotoxigenic *Escherichia coli* Vaccines, 2011:pp. 1–40.

[9] Svennerholm AM, Tobias J. Vaccines against enterotoxigenic *Escherichia coli*. Exp Rev Vacc 2008;7:795–804. https://doi.org/10.1586/14760584.7.6.795.

[10] Bourgeois AL, Wierzba TF, Walker RI. Status of vaccine research and development for enterotoxigenic *Escherichia coli*. Vaccine 2016;34:2880–6. https://doi.org/10.1016/j.vaccine.2016.02.076.

[11] Nataro JP, Kaper JB. Diarrheagenic *Escherichia coli*. Clin Microbiol Rev 1998;1(1):142–201.

[12] Zegeye ED, Govasli ML, Sommerfelt H, Puntervoll P. Development of an enterotoxigenic *Escherichia coli* vaccine based on the heat-stable toxin. Hum Vaccin Immunother 2018:1–10. https://doi.org/10.1080/21645515.2018.1496768.

[13] Kotloff KL, Nataro JP, Blackwelder WC, Nasrin D, Farag TH, Panchalingam S, et al. Burden and aetiology of diarrhoeal disease in infants and young children in developing countries (the global enteric multicenter study, GEMS): a prospective, case-control study. Lancet 2013;382:209–22. https://doi.org/10.1016/S0140-6736(13)60844–2.

[14] Brierley SM. Guanylate cyclase-C receptor activation: unexpected biology. Curr Opin Pharmacol 2012;12:632–40. https://doi.org/10.1016/j.coph.2012.10.005.
[15] Arshad N, Visweswariah SS. The multiple and enigmatic roles of guanylyl cyclase C in intestinal homeostasis. FEBS Lett 2012;586:2835–40. https://doi.org/10.1016/j.febslet.2012.07.028.
[16] Taxt A, Aasland R, Sommerfelt H, Nataro J, Puntervoll P. Heat-stable enterotoxin of enterotoxigenic *Escherichia coli* as a vaccine target. Infect Immun 2010;78:1824–31. https://doi.org/10.1128/IAI.01397-09.
[17] Taxt AM, Diaz Y, Bacle A, Grauffel C, Reuter N, Aasland R, et al. Characterization of immunological cross-reactivity between enterotoxigenic *Escherichia coli* heat-stable toxin and human guanylin and uroguanylin. Infect Immun 2014;82:2913–22. https://doi.org/10.1128/IAI.01749-14.
[18] Taxt AM, Diaz Y, Aasland R, Clements JD, Nataro JP, Sommerfelt H, et al. Towards rational design of a toxoid vaccine against the heat-stable toxin of *Escherichia coli*. Infect Immun 2016;84:1239–49. https://doi.org/10.1128/IAI.01225-15.
[19] Diaz Y, Govasli ML, Zegeye ED, Sommerfelt H, Steinsland H, Puntervoll P. Immunizations with enterotoxigenic *Escherichia coli* heat-stable toxin conjugates engender toxin-neutralizing antibodies in mice that also cross-react with guanylin and uroguanylin. Infect Immun 2019;87(7). https://doi.org/10.1128/IAI.00099-19.
[20] Govasli ML, Diaz Y, Zegeye ED, Darbakk C, Taxt AM, Puntervoll P. Purification and characterization of native and vaccine candidate mutant enterotoxigenic *Escherichia coli* heat-stable toxins. Toxins (Basel) 2018;10:274. https://doi.org/10.3390/toxins10070274.
[21] De Mol P, Hemelhof W, Retoré P, Takeda T, Miwatani T, Takeda Y, et al. A competitive immunosorbent assay for the detection of heat-stable enterotoxin of *Escherichia coli*. J Med Microbiol 1985;20:69–74. https://doi.org/10.1099/00222615-20-1-69.
[22] Zeng W, Azzopardi K, Hocking D, Wong CY, Robevska G, Tauschek M, et al. A totally synthetic lipopeptide-based self-adjuvanting vaccine induces neutralizing antibodies against heat-stable enterotoxin from enterotoxigenic *Escherichia coli*. Vaccine 2012;30:4800–6. https://doi.org/10.1016/j.vaccine.2012.05.017.
[23] Frietze KM, Peabody DS, Chackerian B. Engineering virus-like particles as vaccine platforms. Curr Opin Virol 2016;18:44–9. https://doi.org/10.1016/j.coviro.2016.03.001.
[24] Brune KD, Howarth M. New routes and opportunities for modular construction of particulate vaccines: stick, click, and glue. Front Immunol 2018;9:1432. https://doi.org/10.3389/fimmu.2018.01432.
[25] Bachmann MF, Zinkernagel RM. Neutralizing antiviral B cell responses. Annu Rev Immunol 1997;15:235–70. https://doi.org/10.1146/annurev.immunol.15.1.235.
[26] Dintzis HM, Dintzis RZ, Vogelstein B. Molecular determinants of immunogenicity: the immunon model of immune response. Proc Natl Acad Sci USA 1976;7(3):3671–5.
[27] Bachmann MF, Rohrer UH, Kündig TM, Bürki K, Hengartner H, Zinkernagel RM. The influence of antigen organization on B cell responsiveness. Science 1993;2(62):1448–51.
[28] Jegerlehner A, Storni T, Lipowsky G, Schmid M, Pumpens P, Bachmann MF. Regulation of IgG antibody responses by epitope density and CD21-mediated costimulation. Eur J Immunol 2002;32:3305–14. https://doi.org/10.1002/1521-4141(200211)32:11<3305::AID-IMMU3305>3.0.CO;2-J.
[29] López-Sagaseta J, Malito E, Rappuoli R, Bottomley MJ. Self-assembling protein nanoparticles in the design of vaccines. Comput Struct Biotechnol J 2016;14:58–68. https://doi.org/10.1016/j.csbj.2015.11.001.
[30] Jain NK, Sahni N, Kumru OS, Joshi SB, Volkin DB, Russell Middaugh C. Formulation and stabilization of recombinant protein based virus-like particle vaccines. Adv Drug Deliv Rev 2015;93:42–55. https://doi.org/10.1016/j.addr.2014.10.023.
[31] Jeong H, Seong BL. Exploiting virus-like particles as innovative vaccines against emerging viral infections. J Microbiol 2017;55:220–30. https://doi.org/10.1007/s12275-017-7058-3.
[32] Yan D, Wei Y-Q, Guo H-C, Sun S-Q. The application of virus-like particles as vaccines and biological vehicles. Appl Microbiol Biotechnol 2015;99:10415–32. https://doi.org/10.1007/s00253-015-7000-8.
[33] Kushnir N, Streatfield SJ, Yusibov V. Virus-like particles as a highly efficient vaccine platform: diversity of targets and production systems and advances in clinical development. Vaccine 2012;31:58–83. https://doi.org/10.1016/j.vaccine.2012.10.083.
[34] Zakeri B, Fierer JO, Celik E, Chittock EC, Schwarz-Linek U, Moy VT, et al. Peptide tag forming a rapid covalent bond to a protein, through engineering a bacterial adhesin. Proc Natl Acad Sci USA 2012;109:E690–7. https://doi.org/10.1073/pnas.1115485109.
[35] Brune KD, Leneghan DB, Brian IJ, Ishizuka AS, Bachmann MF, Draper SJ, et al. Plug-and-display: decoration of virus-like particles via isopeptide bonds for modular immunization. Sci Rep 2016;6:19234. https://doi.org/10.1038/srep19234.
[36] Thrane S, Janitzek CM, Matondo S, Resende M, Gustavsson T, de Jongh WA, et al. Bacterial superglue enables easy development of efficient virus-like particle based vaccines. J Nanobiotechnology 2016;14:30. https://doi.org/10.1186/s12951-016-0181-1.
[37] Kapust RB, Tözsér J, Copeland TD, Waugh DS. The P1′ specificity of tobacco etch virus protease. Biochem Biophys Res Commun 2002;294:949–55. https://doi.org/10.1016/S0006-291X(02)00574-0.
[38] Klint JK, Senff S, Saez NJ, Seshadri R, Lau HY, Bende NS, et al. Production of recombinant disulfide-rich venom peptides for structural and functional analysis via expression in the periplasm of *E. coli*. PLoS ONE 2013;8. https://doi.org/10.1371/journal.pone.0063865.
[39] Aida Y, Pabst MJ. Removal of endotoxin from protein solutions by phase separation using Triton X-114. J Immunol Methods 1990;1(32):191–5.
[40] Ritz C, Streibig JC. Bioassay analysis using R. J Stat Softw 2005;12.
[41] Klipstein F, Engert R, Clements J, Houghten R. Protection against human and porcine enterotoxigenic strains of *Escherichia coli* in rats immunized with a cross-linked toxoid vaccine. Infect Immun 1983;40:924–9.
[42] Frederick DR, Goggins JA, Sabbagh LM, Freytag LC, Clements JD, McLachlan JB. Adjuvant selection regulates gut migration and phenotypic diversity of antigen-specific CD4+ T cells following parenteral immunization. Mucosal Immunol 2018;11:549–61. https://doi.org/10.1038/mi.2017.70.
[43] Naylor C, Lu M, Haque R, Mondal D, Buonomo E, Nayak U, et al. Environmental enteropathy, oral vaccine failure and growth faltering in infants in Bangladesh. EBioMedicine 2015;2:1759–66. https://doi.org/10.1016/j.ebiom.2015.09.036.